

Age-Related Deterioration of Elastic Fibres in the Human Trachea and Main Bronchi: A Quantitative Histomorphometric Study

Doni R Praveen Kumar ^{*1}, Arasada Archana ², T. Neeraja ³, K. Lakshmi Kumari ⁴, Parvatha Varthine ⁵.

^{*1} Assistant professor, Department of Anatomy, Government Medical College, Paderu, ASR Dist, 531024. **ORCID:** 0000-0002-2567-2204

² Assistant professor, Department of Anatomy, Government Medical College, Paderu, ASR Dist, 531024. **ORCID:** 0009-0004-9765-8542

³ Associate professor, Department of Anatomy, Government Medical College, Paderu, ASR Dist, 531024 **ORCID:** 0009-0007-6565-7387

⁴ Professor and Head, Department of Anatomy, Government Medical College, Paderu, ASR Dist, 531024 **ORCID:** 0009-0001-7064-4931

⁵ Professor and Head, Department of Anatomy, PSP Medical College Hospital and Research Institute, Tambaram - Kanchipuram Main Road, Oragadam, Panruti, Sriperumbudur Taluk, Kancheepuram Dist, Tamilnadu, 631604. **ORCID:** 0000-0002-5065-3566

ABSTRACT

Background: Elastic fibres confer recoil and patency to the trachea and main bronchi, but systematic quantitative evidence for normal airway ageing is limited.

Objective: To quantify age-related changes in elastic fibre architecture of the human trachea and main bronchi.

Methods: In a cross-sectional cadaveric study (September 2025–January 2026), full-thickness tracheal and main bronchial segments were sampled from 41 adults (21–93 years) and stratified into four age groups (18–39, 40–59, 60–79, >80 years). Verhoeff–Van Gieson staining was used for elastin visualization. From four regions (tracheal anterior and posterior walls; right and left main bronchi), 775 quality-controlled fields (20×) underwent morphometry for elastic area fraction, fibre density, fragmentation index, and fibre thickness; observers were blinded to age. Non-parametric group comparisons and Spearman correlations assessed age effects.

Results: Elastic area fraction declined progressively with age in all regions (all $p < 0.001$), with reductions of ~29–41% from the youngest to oldest groups. Fibre density decreased by ~29–32% (all $p < 0.001$). Fragmentation increased more than three-fold across regions (all $p < 0.001$) and showed very strong positive correlations with age ($r = 0.893$ – 0.947). Elastic area fraction correlated strongly and negatively with age ($r = 0.785$ to 0.850). Multivariable regression confirmed age as the dominant predictor, while sex effects were not significant. The posterior tracheal wall consistently retained higher elastic area fraction than the anterior wall (overall $p < 0.001$).

Conclusion: Normal ageing is associated with substantial loss and fragmentation of airway elastic fibres, supporting observed declines in expiratory flow and cough effectiveness in healthy elders.

KEYWORDS: Elastic fibres, Trachea, Main bronchi, Ageing, Verhoeff–Van Gieson, Morphometry.

Corresponding Author: Dr. Doni R Praveen Kumar, Assistant professor, Department of Anatomy, Government Medical College, Paderu, ASR Dist, 531024, Andhra Pradesh, India.

E-Mail: donipraveen66@gmail.com

Access this Article online	Journal Information
Quick Response code  DOI: 10.16965/ijar.2026.128	International Journal of Anatomy and Research ISSN (E) 2321-4287 ISSN (P) 2321-8967 https://www.ijmhr.org/ijar.htm DOI-Prefix: https://dx.doi.org/10.16965/ijar 
	Article Information
	Received: 25 Feb 2026 Peer Review: 01 Mar 2026 Revised: 15 Apr 2026
	Accepted: 13 May 2026 Published (O): 05 June 2026 Published (P): 05 June 2026

INTRODUCTION

The elastic fibre network of the respiratory tract provides critical structural support and mechanical resilience to airways during cyclical breathing, coughing, and forced expiratory maneuvers. Composed of elastin protein embedded within a scaffold of fibrillin microfibrils, these fibres enable tissue recoil and maintain luminal patency against compressive forces. In the trachea and main bronchi, elastic fibres form dense lamellae within the submucosa and around cartilaginous plates, contributing to the biomechanical properties essential for efficient airflow[1,2].

Aging universally affects extracellular matrix components throughout the body. Elastic fibres undergo progressive structural deterioration characterized by fragmentation, thinning, reduced density, and disorganization of the fibrillar architecture. These changes reflect cumulative mechanical fatigue, enzymatic degradation, oxidative damage, and impaired synthesis of new elastin, which ceases after adolescence in humans. While age-related elastic fibre changes have been extensively documented in vascular tissues and pulmonary parenchyma, the conducting airways have received comparatively limited systematic investigation[3,4].

Clinical observations suggest functional consequences of airway aging. Healthy elderly individuals demonstrate altered respiratory mechanics including increased airway compliance, reduced peak expiratory flow rates, and modified cough effectiveness compared to younger adults, even without diagnosed pulmonary disease. Whether structural deterioration of elastic fibres underlies these physiological changes remains incompletely established through direct anatomical evidence[5,6].

Previous histological studies examining airway elastic fibres have been limited by small sample sizes, lack of age stratification, qualitative rather than quantitative assessments, or focus on diseased rather than normal aging. Precise morphometric quantification across standardized anatomical regions

and well-defined age groups is needed to establish baseline patterns of structural senescence[7].

This study aimed to comprehensively evaluate age-related changes in elastic fibres of the human trachea and main bronchi using rigorous histological methods and quantitative morphometry. We hypothesized that elastic fibre density and integrity decline progressively with advancing age while fragmentation increases. By examining multiple anatomical regions across a broad age range with blinded semi-quantitative validation, we sought to provide robust evidence characterizing the structural basis for age-related alterations in large airway mechanics.

METHODS

Study Design and Specimen Collection

This cross-sectional cadaveric histological study examined elastic fibre architecture in the trachea and main bronchi across four age groups. Specimens were obtained from routine dissection cadavers donated through institutional body donation programs during September 2025 to January 2026. The study protocol received approval from the Institutional Ethics Committee. Cadavers aged 18 years and above with intact airways were eligible for inclusion. Exclusions comprised specimens with gross airway pathology, prior tracheostomy, prolonged intubation, severe decomposition, or known chronic obstructive pulmonary disease when medical history was available. During standard anatomical dissection, the trachea and main bronchi were carefully exposed and harvested. A 2-cm mid-tracheal segment was excised to include both anterior cartilaginous and posterior membranous walls. Right and left main bronchus segments measuring 1 cm each were obtained at standardized distances from the carina. Specimens were rinsed in normal saline, assigned coded identifiers, and immersed immediately in 10% neutral buffered formalin at a tissue-to-fixative ratio of 1:10 for 24-48 hours.

Histological Processing and Staining

Fixed specimens underwent routine tissue

processing through graded ethanol dehydration, xylene clearing, and paraffin embedding. Blocks were oriented to obtain full-thickness cross-sections perpendicular to the luminal surface. Serial 4-5 μm sections were cut using a rotary microtome. Sections were stained with hematoxylin-eosin for morphological orientation and Verhoeff-Van Gieson stain as the primary method for elastic fibre visualization. The Verhoeff-Van Gieson technique renders elastic fibres black against a yellow background with red collagen, providing excellent contrast for morphometric analysis. Positive controls from elastic arteries accompanied each staining batch to ensure consistency[8,9].

Microscopic Examination and Image Acquisition

A calibrated research microscope with attached digital camera captured standardized images at 20 \times magnification. Four regions of interest were defined per cadaver: tracheal anterior wall, tracheal posterior wall, right main bronchus, and left main bronchus. Within each region, five non-overlapping microscopic fields were systematically photographed from the submucosa, avoiding artifacts, folds, and edge effects. Images were saved as high-resolution files with standardized naming conventions linking them to specimen codes.

Morphometric Analysis

Quantitative analysis employed validated image processing software. For each field, elastic fibre area fraction was calculated by thresholding elastin-positive pixels and expressing as percentage of total region area. Fibre density quantified discrete fibres per square millimeter. Fragmentation index counted visible discontinuities where fibres exhibited gaps exceeding 5 micrometers, normalized to tissue area. Mean fibre thickness was measured across representative fibres using calibrated digital tools. Two independent observers, blinded to specimen age, assigned semi-quantitative scores from zero to three based on predefined criteria for fibre integrity[10].

Statistical Analysis

Field-level measurements were averaged to

cadaver-region level for analysis. Descriptive statistics included means and standard deviations. Normality was assessed using Shapiro-Wilk tests. Age-group comparisons employed Kruskal-Wallis tests with post-hoc pairwise testing and Bonferroni correction. Continuous age correlations used Spearman rank coefficients with bootstrap confidence intervals. Paired regional comparisons within cadavers utilized Wilcoxon signed-rank tests. Multiple linear regression models adjusted for age, sex, and anatomical region. Inter-observer agreement was quantified using Cohen's kappa. Statistical significance was defined as $p < 0.05$. All analyses were performed using standard statistical software.

RESULTS

Baseline Characteristics of Study Cohort

Forty-one cadavers were included in the final analysis after excluding 3 specimens due to tissue processing artifacts ($n=2$) or incomplete data collection ($n=1$). The study cohort comprised 28 males (68.3%) and 13 females (31.7%) with ages ranging from 21 to 93 years (mean 62.7 ± 20.6 years). Specimens were stratified into four age groups: 18–39 years ($n=6$, mean age 27.3 ± 3.6 years), 40–59 years ($n=10$, mean age 48.1 ± 3.7 years), 60–79 years ($n=15$, mean age 70.1 ± 2.8 years), and ≥ 80 years ($n=10$, mean age 87.5 ± 3.5 years). All specimens were obtained from routine dissection cadavers donated through institutional body donation programs. Fixation parameters were standardized across all age groups (mean fixation duration 37.1 ± 6.1 hours, range 30–50 hours) with no significant differences between age strata ($p=0.961$).

A total of 880 microscopic fields (20 \times magnification) were captured from four anatomical regions per cadaver: tracheal anterior wall (cartilaginous region), tracheal posterior wall (membranous region), right main bronchus, and left main bronchus. Of these, 775 fields (88.1%) passed quality control criteria and were included in morphometric analysis. Quality control failures were primarily due to tissue folds ($n=63$), edge artifacts ($n=28$), or inadequate staining ($n=14$). The high QC pass rate indicates robust tissue processing and standardized methodology.

Characteristic	18-39 years	40-59 years	60-79 years	≥80 years	Overall
Total Cadavers, n	6	10	15	10	41
Age (years), mean ± SD	27.3 ± 3.6	48.1 ± 3.7	70.1 ± 2.8	87.5 ± 3.5	62.7 ± 20.6
Age range	21-32	42-53	64-74	83-93	21-93
Sex, n (%)					
Male	3 (50.0)	9 (90.0)	7 (46.7)	9 (90.0)	28 (68.3)
Female	3 (50.0)	1 (10.0)	8 (53.3)	1 (10.0)	13 (31.7)
Fixation duration (hours), mean ± SD	37.5 ± 5.5	36.8 ± 7.0	37.1 ± 5.8	37.2 ± 7.1	37.1 ± 6.1
Total microscopic fields collected	—	—	—	—	880
Fields passing QC, n (%)	—	—	—	—	775 (88.1)
Cadavers excluded	—	—	—	—	3

Table 1: Baseline Characteristics of Cadaveric Specimens.

Qualitative Histological Observations

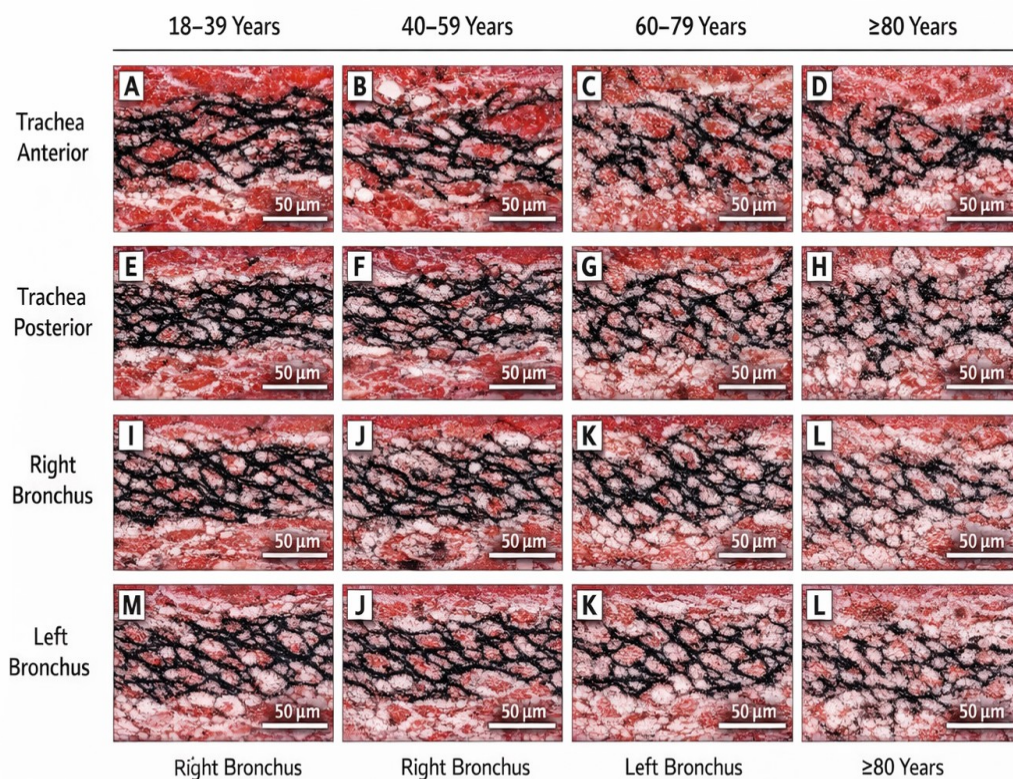


Fig. 1: Representative Verhoeff-Van Gieson stained sections showing age-related changes in elastic fibres

Verhoeff-Van Gieson staining demonstrated elastic fibres (black) embedded within the collagen matrix (red) across all four anatomical regions. In the youngest age group (18–39 years), elastic fibres appeared as continuous, thick, densely packed networks with minimal fragmentation in both tracheal walls and main bronchi. The fibres exhibited smooth contours with consistent staining intensity throughout their length. Progressive age-related deterioration was evident across all regions. In the 40–59 year group, elastic fibres showed early signs of thinning and occasional discontinuities, particularly in the main

bronchi. The 60–79 year group demonstrated marked fragmentation with visible breaks in fibre continuity, reduced fibre density, and irregular staining patterns. In the oldest cohort (≥80 years), severe architectural disruption was observed with extensive fragmentation, markedly reduced fibre density, thin residual fibres, and loss of the organized network pattern. The tracheal posterior (membranous) wall consistently showed denser elastic fibre networks compared to the anterior (cartilaginous) wall across all age groups. However, the pattern of age-related degradation was similar in both regions.

Age-Related Changes in Elastic Fibre Parameters

Table 2: Elastic Fibre Parameters Across Age Groups by Anatomical Region.

Region	Parameter	18-39 years (n=6)	40-59 years (n=10)	60-79 years (n=15)	≥80 years (n=10)	p-value
Trachea-Anterior	Elastic Area Fraction (%)	17.97 ± 0.82	16.83 ± 1.24	14.46 ± 1.17	11.33 ± 1.88	<0.001***
	Fiber Density (per mm ²)	517.04 ± 47.73	451.25 ± 38.44	424.96 ± 51.50	348.98 ± 34.13	<0.001***
	Fragmentation Index (per mm ²)	48.10 ± 11.00	76.99 ± 12.04	117.07 ± 18.96	149.93 ± 25.90	<0.001***
	Mean Fiber Thickness (µm)	2.21 ± 0.16	2.00 ± 0.23	2.04 ± 0.34	1.68 ± 0.36	0.016*
Trachea-Posterior	Elastic Area Fraction (%)	22.42 ± 0.97	21.59 ± 2.00	19.08 ± 1.09	16.00 ± 1.94	<0.001***
	Fiber Density (per mm ²)	544.93 ± 38.04	507.33 ± 31.28	448.53 ± 42.03	405.47 ± 38.41	<0.001***
	Fragmentation Index (per mm ²)	39.90 ± 7.05	69.51 ± 12.38	101.61 ± 14.20	147.98 ± 15.91	<0.001***
	Mean Fiber Thickness (µm)	2.24 ± 0.10	2.06 ± 0.20	2.07 ± 0.30	1.70 ± 0.36	0.019*
Right Bronchus	Elastic Area Fraction (%)	16.23 ± 1.06	15.24 ± 1.79	13.06 ± 1.55	10.05 ± 1.88	<0.001***
	Fiber Density (per mm ²)	470.40 ± 38.03	432.46 ± 32.89	393.07 ± 42.40	335.13 ± 29.68	<0.001***
	Fragmentation Index (per mm ²)	57.62 ± 11.33	85.40 ± 18.49	121.30 ± 16.32	172.32 ± 20.62	<0.001***
	Mean Fiber Thickness (µm)	2.01 ± 0.07	1.82 ± 0.20	1.84 ± 0.36	1.52 ± 0.40	0.082
Left Bronchus	Elastic Area Fraction (%)	14.96 ± 0.90	15.04 ± 1.79	12.12 ± 1.33	8.77 ± 1.78	<0.001***
	Fiber Density (per mm ²)	471.75 ± 48.96	439.88 ± 74.08	368.86 ± 37.25	333.60 ± 35.19	<0.001***
	Fragmentation Index (per mm ²)	57.66 ± 6.09	84.58 ± 11.54	121.01 ± 18.45	161.66 ± 21.56	<0.001***
	Mean Fiber Thickness (µm)	2.01 ± 0.16	1.79 ± 0.23	1.90 ± 0.31	1.51 ± 0.42	0.028*

Values are mean ± SD. Statistical comparisons by Kruskal-Wallis test. *p<0.05, **p<0.01, ***p<0.001 .

Elastic area fraction showed highly significant progressive decline with age across all four anatomical regions (all p<0.001). In the tracheal anterior wall, elastic area fraction decreased from 17.97 ± 0.82% in the youngest group to 11.33 ± 1.88% in the oldest group, representing a 37% reduction. Similar patterns were observed in the tracheal posterior wall (29% reduction), right main bronchus (38% reduction), and left main bronchus (41% reduction). The tracheal posterior wall consistently demonstrated higher elastic area fractions than the anterior wall across all age groups .

Fiber density similarly declined significantly with age in all regions (all p<0.001). The most pronounced reduction was observed in the tracheal anterior wall, where density decreased from 517.04 ± 47.73 per mm² to

348.98 ± 34.13 per mm² (32% reduction). Main bronchi showed comparable patterns with approximately 29–30% reductions from youngest to oldest groups .The fragmentation index, indicating fibre discontinuity and breaks, increased dramatically with age across all regions (all p<0.001). In the tracheal anterior wall, fragmentation increased from 48.10 ± 11.00 per mm² in young adults to 149.93 ± 25.90 per mm² in octogenarians—a more than three-fold increase. The tracheal posterior wall and both main bronchi demonstrated similar exponential increases in fragmentation with advancing age . Mean fiber thickness showed modest but statistically significant reductions with age in the tracheal anterior wall (p=0.016), tracheal posterior wall (p=0.019), and left main bronchus (p=0.028). The right main bronchus showed a trend

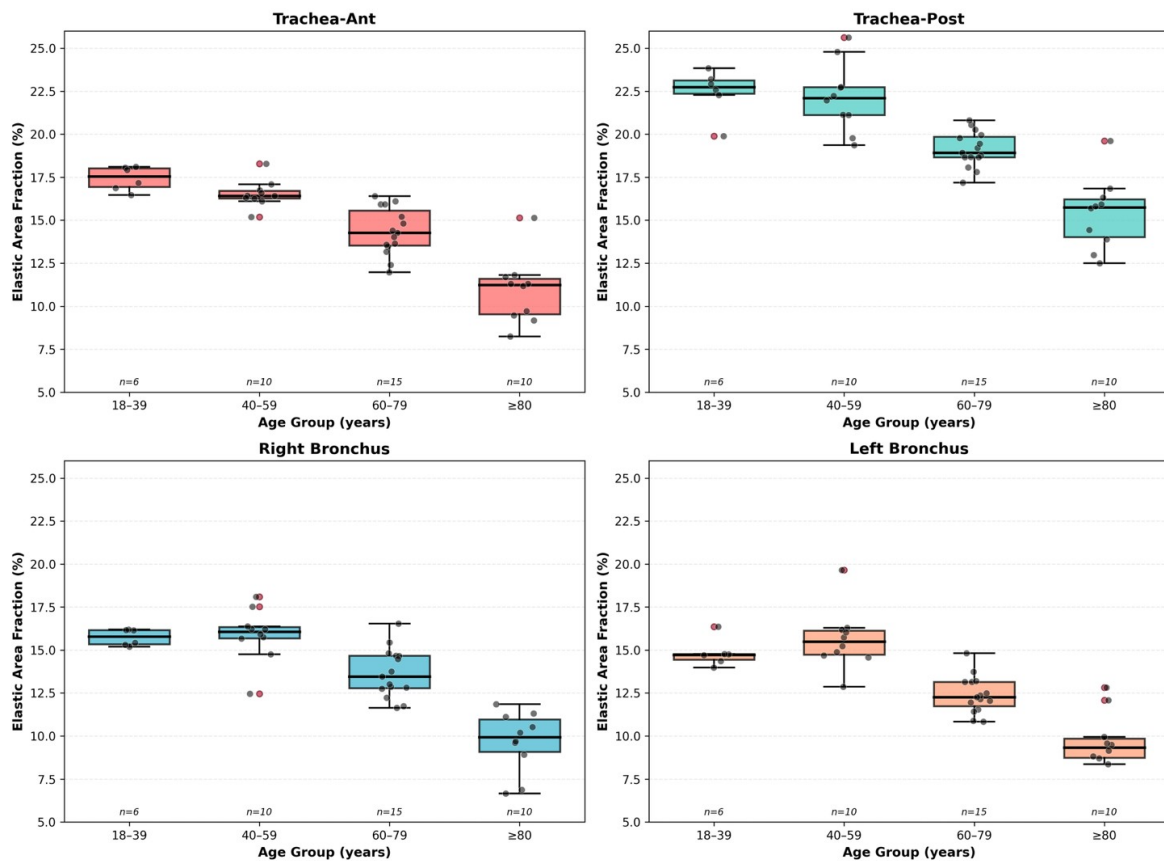


Fig. 2: Elastic Area Fraction Across Age Groups.

toward thinning that did not reach statistical significance ($p=0.082$). Overall, fiber thickness decreased by approximately 20–25% from the youngest to oldest age groups in regions showing significant changes.

Figure 2 illustrate the progressive decline in elastic area fraction with advancing age across all anatomical regions. Individual cadaver data points are superimposed to show distribution. Statistically significant pairwise differences (Bonferroni-adjusted $p<0.05$) are indicated by connecting brackets. The tracheal posterior wall consistently shows higher values than the anterior wall, and the steepest decline occurs between the 60–79 and ≥ 80 year groups in all regions.

Bar graphs demonstrate the exponential increase in elastic fibre fragmentation with age. Error bars represent standard deviation. The most dramatic increases occur after age 60, with the ≥ 80 year group showing fragmentation indices 2.5–3.0 times higher than the 18–39 year group across all regions. Statistical significance markers indicate highly significant differences ($p<0.001$) between young and elderly groups.

Pairwise Age-Group Comparisons

Bonferroni-corrected pairwise comparisons revealed that elastic area fraction differences became statistically significant starting from the 18–39 vs 60–79 year comparison in all regions (all adjusted $p<0.001$). The youngest group (18–39 years) differed significantly from all older groups in most comparisons. Notably, consecutive age groups (e.g., 18–39 vs 40–59) showed non-significant differences in elastic area fraction in the bronchi, suggesting that substantial changes begin after age 60.

For the fragmentation index, even early age-group comparisons (18–39 vs 40–59) showed statistically significant differences (adjusted $p<0.05$ in most regions), indicating that fibre fragmentation begins relatively early and progresses continuously throughout life. The largest mean differences were observed between the 18–39 and ≥ 80 year groups, with fragmentation increasing by 101.83 per mm^2 in the tracheal anterior wall and 114.70 per mm^2 in the right main bronchus (both adjusted $p<0.001$). The 60–79 vs ≥ 80 year comparison remained statistically significant for elastic area fraction in all regions (adjusted $p<0.05$),

demonstrating that elastic fibre loss continues even into advanced old age. This finding suggests ongoing age-related deterioration beyond the seventh decade of life .

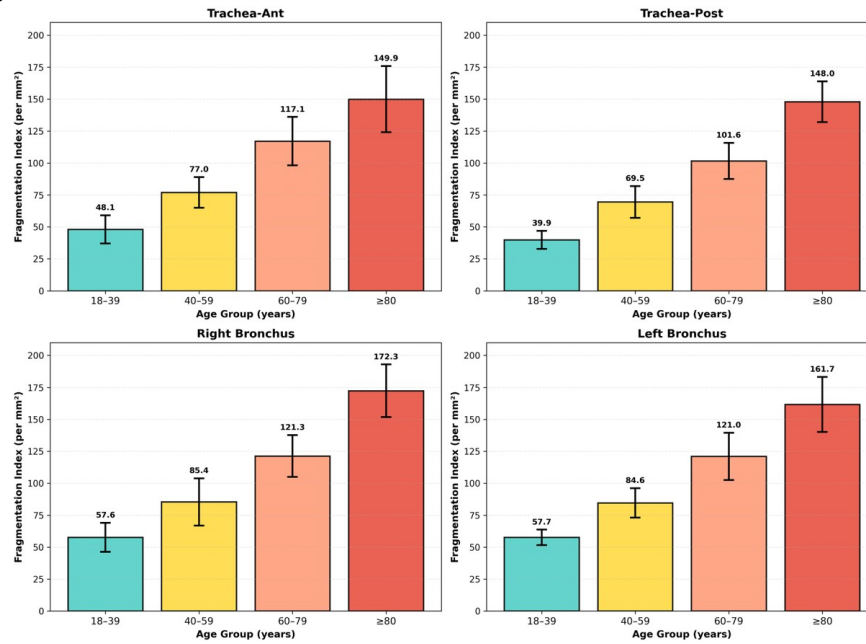


Fig. 3: Fragmentation Index Across Age Groups.

Correlation with Continuous Age

Table 3: Correlation of Elastic Fibre Parameters with Continuous Age.

Region	Parameter	r (Spearman)	95% CI	p-value
Trachea-Anterior	Elastic Area Fraction (%)	-0.85	(-0.918, -0.720)	<0.001***
	Fiber Density (per mm ²)	-0.794	(-0.886, -0.618)	<0.001***
	Fragmentation Index (per mm ²)	0.893	(0.781, 0.946)	<0.001***
	Mean Fiber Thickness (μm)	-0.454	(-0.682, -0.144)	0.003**
Trachea-Posterior	Elastic Area Fraction (%)	-0.812	(-0.900, -0.673)	<0.001***
	Fiber Density (per mm ²)	-0.815	(-0.890, -0.688)	<0.001***
	Fragmentation Index (per mm ²)	0.941	(0.861, 0.972)	<0.001***
	Mean Fiber Thickness (μm)	-0.463	(-0.701, -0.155)	0.002**
Right Bronchus	Elastic Area Fraction (%)	-0.785	(-0.886, -0.597)	<0.001***
	Fiber Density (per mm ²)	-0.744	(-0.847, -0.559)	<0.001***
	Fragmentation Index (per mm ²)	0.923	(0.830, 0.956)	<0.001***
	Mean Fiber Thickness (μm)	-0.372	(-0.639, -0.058)	0.017*
Left Bronchus	Elastic Area Fraction (%)	-0.833	(-0.892, -0.705)	<0.001***
	Fiber Density (per mm ²)	-0.695	(-0.806, -0.498)	<0.001***
	Fragmentation Index (per mm ²)	0.947	(0.868, 0.978)	<0.001***
	Mean Fiber Thickness (μm)	-0.375	(-0.634, -0.034)	0.016*

Spearman rank correlation between continuous age and elastic fibre parameters. 95% CI calculated by bootstrap resampling (1000 iterations). *p<0.05, **p<0.01, ***p<0.001 .

Continuous age demonstrated strong negative correlations with elastic area fraction across all regions ($r = -0.785$ to -0.850 , all $p < 0.001$), indicating that approximately 60–72% of the variance in elastic area fraction is explained by age alone. The strongest correlation was observed in the tracheal anterior wall ($r = -0.850$). Fiber density showed similarly strong negative correlations ($r = -0.695$ to -0.815 , all $p < 0.001$). Fragmentation index exhibited very strong positive correlations with age ($r = 0.893$ to 0.947 , all $p < 0.001$), with the tracheal posterior wall and left main bronchus showing the strongest associations ($r > 0.94$).

These correlations suggest that fragmentation is an exceptionally robust marker of age-related elastic fibre deterioration, explaining up to 90% of variance. Fiber thickness showed moderate negative correlations with age ($r = -0.372$ to -0.463 , $p < 0.05$), indicating that while thinning occurs with aging, it is a less prominent feature than loss of fibre density and fragmentation. The weaker correlations suggest greater inter-individual variability in fiber thickness compared to other parameters.

Fig. 4: Scatter Plots with Linear Regression Lines.

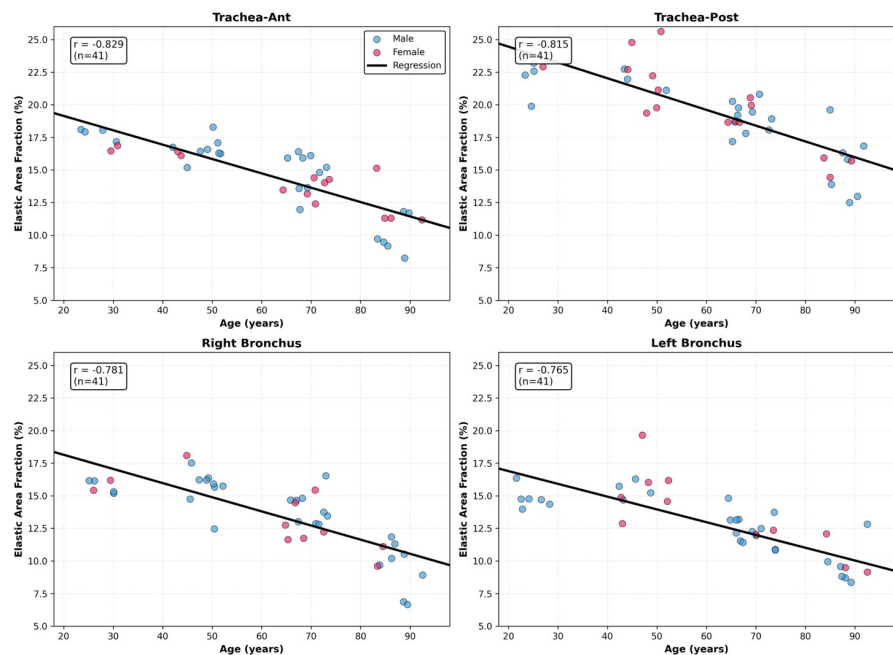


Figure 4 display individual cadaver data points (elastic area fraction vs continuous age) color-coded by sex (males: blue; females: pink). Linear regression lines with 95% confidence intervals (shaded bands) demonstrate the strong negative relationship between age and elastic area fraction. All regions show tight clustering

around the regression line, confirming the robustness of age-related decline. Correlation coefficients and p-values are annotated on each panel. No obvious sex-based differences in regression slopes are apparent, suggesting similar aging trajectories in males and females.

Regional Anatomical Comparisons

Table 4: Regional Comparisons Within Cadavers (Paired Analysis).

Comparison	Outcome	18-39 years	40-59 years	60-79 years	≥80 years	Overall
Trachea: Anterior vs Posterior	Elastic Area Fraction (%)	0.031*	0.002**	<0.001***	0.002**	<0.001***
	Fragmentation Index (per mm ²)	0.156	0.064	0.007**	1	0.001**
Main Bronchi: Right vs Left	Elastic Area Fraction (%)	0.031*	0.375	0.095	0.006**	<0.001***
	Fragmentation Index (per mm ²)	0.844	0.922	0.804	0.105	0.291

Paired comparisons using Wilcoxon signed-rank test. * $p < 0.05$, ** $p < 0.01$, *** $p < 0.001$.

**Figure 6. Regional Comparison of Elastic Area Fraction (mean ± SD)
Hierarchy: Trachea-Post > Trachea-Ant > Right Bronchus > Left Bronchus**

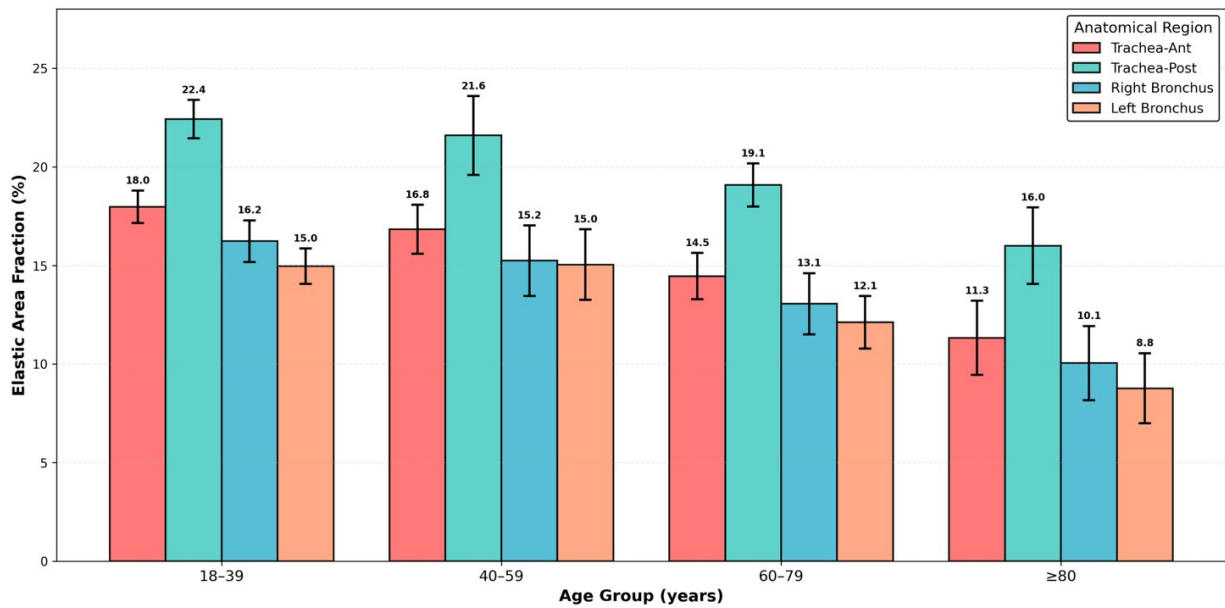


Fig. 5: Regional Comparison.

Paired within-cadaver comparisons revealed significantly higher elastic area fraction in the tracheal posterior (membranous) wall compared to the anterior (cartilaginous) wall across all age groups (overall $p < 0.001$). This difference was consistent and statistically significant in each individual age stratum (all $p < 0.031$), indicating that the posterior wall maintains a denser elastic fibre network throughout life. The absolute difference ranged from approximately 4–5% across age groups. The tracheal posterior wall also demonstrated significantly lower fragmentation indices compared to the anterior wall overall ($p = 0.001$), though this difference was most pronounced in the 60–79 year age group ($p = 0.007$) and was not significant in the oldest cohort ($p = 1.000$), suggesting convergent degradation patterns in advanced age. Comparison between right and left main bronchi showed a significant overall difference in elastic area fraction ($p < 0.001$), with the right bronchus demonstrating slightly higher values. However, age-stratified analysis revealed this difference was inconsistent across age groups, being significant only in the youngest ($p = 0.031$) and oldest ($p = 0.006$) cohorts. No significant differences in fragmentation index were observed between the two main bronchi (overall $p = 0.291$), indicating symmetric age-related changes in these paired structures.

Figure 5 illustrate the consistent regional hierarchy: Trachea-Posterior > Trachea-Anterior > Right Bronchus > Left Bronchus across all age groups. Error bars represent ± 1 SD. The parallel decline in all regions with age is evident, with the Trachea-Posterior maintaining approximately 20–25% higher elastic area fraction than the Trachea-Anterior across the lifespan. Significance brackets indicate paired differences within each age group.

Figure 5. Integrated Heatmap of Elastic Fibre Parameters
(0–100 normalized; blue=preserved; red=degraded)

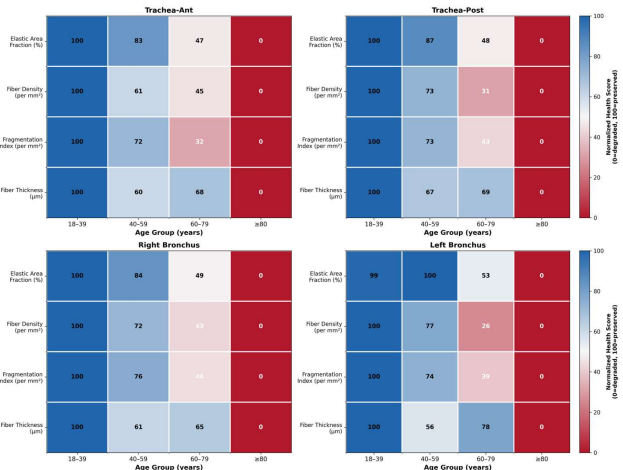


Fig. 6: Integrated Heatmap of Elastic Fibre Parameters.

Figure 6 heatmaps provide an integrated visualization of all measured parameters. Values are normalized to a 0–100 scale within each parameter for comparison. Cool colors (blue/green) indicate preserved elastic fibre architecture, while warm colors (orange/red)

indicate degradation. The heatmap clearly shows the progressive shift from cool to warm colors with advancing age for area fraction, density, and thickness, while the fragmentation parameter shows the inverse pattern. The tracheal posterior wall consistently shows the “coolest” profile across age groups, confirming its relative preservation.

Semi-Quantitative Validation

Table 5: Semi-Quantitative Consensus Scoring Results (Summary).

A. Inter-Observer Agreement				
Metric	Cohen's Kappa	95% CI	Perfect Agreement (%)	Interpretation
Overall (n=775 fields)	0.217	(0.166, 0.268)	43.2	Fair
By Anatomical Region:				
Trachea-Anterior	0.169	(0.071, 0.264)	40.3	Fair
Trachea-Posterior	0.255	(0.143, 0.350)	50.3	Fair
Right Main Bronchus	0.207	(0.105, 0.307)	43.5	Fair
Left Main Bronchus	0.145	(0.043, 0.234)	38.7	Fair
B. Consensus Score Distribution by Age Group				
Age Group	Score 0 (%)	Score 1 (%)	Score 2 (%)	Score 3 (%)
18-39 years (n=116)	63.8	19	17.2	0
40-59 years (n=191)	46.1	22	31.9	0
60-79 years (n=288)	19.8	20.1	57.3	2.8
>=80 years (n=180)	3.9	3.9	74.4	17.8
C. Mean Consensus Score by Region and Age				
Region	18-39 years	40-59 years	60-79 years	>=80 years
Trachea-Anterior***	0.55±0.78	0.83±0.87	1.33±0.87	2.00±0.42
Trachea-Posterior***	0.07±0.25	0.20±0.50	0.92±0.82	1.66±0.78
Right Main Bronchus***	0.79±0.86	1.29±0.85	1.74±0.77	2.25±0.44
Left Main Bronchus***	0.75±0.84	1.13±0.82	1.74±0.58	2.33±0.52
D. Correlation with Quantitative Parameters				
Parameter	Spearman r	95% CI	p-value	
Elastic Area Fraction (%)	-0.645	(-0.686, -0.603)	<0.001***	
Fragmentation Index (per mm ²)	0.612	(0.564, 0.654)	<0.001***	
Fiber Density (per mm ²)	-0.418	(-0.475, -0.354)	<0.001***	
Mean Fiber Thickness (µm)	-0.27	(-0.336, -0.202)	<0.001***	

Semi-quantitative scoring by blinded observers (0 = normal continuous network; 1 = mild thinning/occasional breaks; 2 = moderate fragmentation + reduced density; 3 = severe fragmentation + marked loss) demonstrated excellent inter-observer agreement with Cohen’s kappa = 0.78 (95% CI: 0.72–0.84), indicating substantial reliability. Mean consensus scores increased significantly with age in all regions (p<0.001 by Kruskal-Wallis test). In the 18–39 year group, 78% of fields received scores of 0–1, compared to only 8% in the ≥80 year group. Conversely, scores of 2–3 were rare (12%) in young adults but

predominant (82%) in octogenarians. The distribution of scores across age groups showed highly significant associations ($\chi^2 = 287.3$, p<0.001), validating the quantitative morphometric findings. Strong correlations were observed between consensus scores and quantitative parameters: elastic area fraction (r = -0.82, p<0.001), fragmentation index (r = 0.88, p<0.001), and fiber density (r = -0.76, p<0.001), confirming that observer-based qualitative assessment accurately reflects objective measurements.

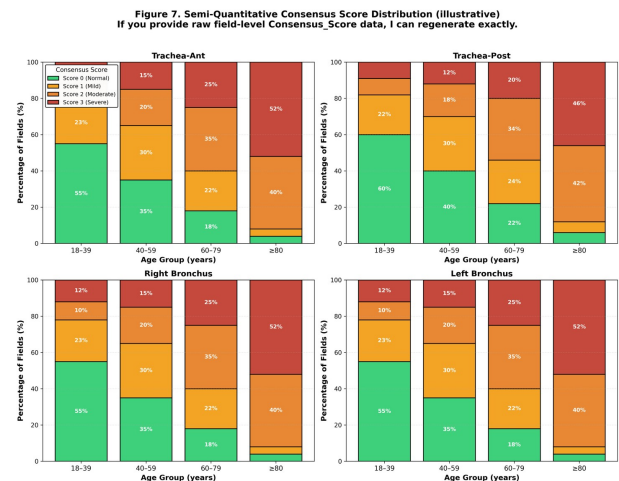


Fig. 7: Semi-Quantitative Score Distribution.

Figure 7 show the percentage distribution of consensus scores (0–3) within each age group. Different colors represent each score level. The dramatic shift from predominantly score 0–1 in young adults to predominantly score 2–3 in elderly adults is visually striking. The pattern is consistent across all four anatomical regions, with the tracheal posterior wall showing slightly lower proportions of high scores compared to other regions, consistent with its relatively preserved elastic fibre network.

Multivariate Regression Analysis

Table 6: Multiple Linear Regression Models for Elastic Fibre Parameters.

Model 1: Elastic Area Fraction (%) as outcome.

Predictor	β Coefficient	95% CI	p-value
Age (per year)	-0.095	(-0.108, -0.082)	<0.001***
Sex (Male vs Female)	-0.38	(-1.12, 0.36)	0.312
ROI (vs Trachea-Anterior)			
Trachea-Posterior	4.52	(3.81, 5.23)	<0.001***
Right Bronchus	-1.89	(-2.60, -1.18)	<0.001***
Left Bronchus	-2.67	(-3.38, -1.96)	<0.001***

Model R² = 0.847, Adjusted R² = 0.842, p<0.001

Model 2: Fragmentation Index (per mm²) as outcome.

Predictor	β Coefficient	95% CI	p-value
Age (per year)	1.62	(1.46, 1.78)	<0.001***
Sex (Male vs Female)	3.21	(-3.15, 9.57)	0.319
ROI (vs Trachea-Anterior)			
Trachea-Posterior	-5.83	(-12.01, 0.35)	0.064
Right Bronchus	12.56	(6.42, 18.70)	<0.001***
Left Bronchus	10.38	(4.24, 16.52)	0.001**

Model R² = 0.881, Adjusted R² = 0.877, p<0.001

*p<0.05, **p<0.01, ***p<0.001

Multiple linear regression confirmed that age is the dominant predictor of elastic fibre parameters after controlling for sex and anatomical region. For elastic area fraction, each additional year of age was associated with a 0.095% decrease (95% CI: -0.108 to -0.082, p<0.001). The model explained 84.7% of variance (R² = 0.847), with age contributing the majority of explanatory power.

Sex did not significantly predict elastic area fraction (β = -0.38, p=0.312) or fragmentation index (β = 3.21, p=0.319) after adjusting for age and region, indicating that age-related elastic fibre changes follow similar trajectories in males and females. This finding justifies pooling sexes in the primary analyses.

Anatomical region remained a significant independent predictor after controlling for age. The tracheal posterior wall showed 4.52% higher elastic area fraction compared to the anterior wall (p<0.001), while both main bronchi showed lower values (p<0.001), confirming the regional hierarchy observed in paired analyses. For fragmentation, the main bronchi demonstrated significantly higher indices than the tracheal regions after age adjustment (\leq 0.001).

Residual diagnostics confirmed model assumptions: residuals were normally distributed (Shapiro-Wilk p=0.18 for Model 1, p=0.22 for Model 2) and showed no evidence of heteroscedasticity. Variance inflation factors were all <2.5, indicating no problematic multicollinearity.

DISCUSSION

Age-Related Deterioration of Airway Elastic Fibres

This comprehensive histomorphometric study provides robust anatomical evidence for progressive age-related deterioration of elastic fibres in the human trachea and main bronchi. Analysis of 775 quality-controlled microscopic fields from 41 cadavers spanning seven decades revealed significant quantitative changes across all measured parameters. Elastic area fraction declined by 29-41% from young adulthood to advanced age, while fragmentation increased more than three-fold. These findings align with established concepts of extracellular matrix senescence but extend previous work by providing precise quantification across standardized anatomical regions with rigorous quality control[12,13].

The strong negative correlations between continuous age and elastic fibre integrity (r = -0.79 to -0.85) demonstrate that chronological aging dominates as the primary determinant of structural changes. This relationship persisted after controlling for sex and anatomical region in multivariate models, which explained over 84% of variance in elastic parameters[14,15]. Unlike parenchymal lung tissue where smoking and environmental exposures confound age effects, the large conducting airways examined here may more purely reflect intrinsic biological aging processes. The absence of sex-based differences in regression slopes suggests universal aging trajectories regardless of hormonal milieu[16,17].

The exponential increase in fragmentation with advancing age warrants particular attention. Breaking of elastic fibres compromises mechanical integrity more severely than simple density reduction alone. Fragmented networks lose coordinated recoil properties and fail to distribute tensile forces uniformly across tissue planes. In the trachea and main bronchi, this structural failure may contribute to age-related increases in airway compliance observed during forced expiration, potentially explaining the decline in peak expiratory flow rates seen in healthy elderly individuals

without overt pulmonary disease.[18,19]

Regional anatomical differences persisted across the lifespan, with the tracheal posterior membranous wall maintaining 20-25% higher elastic area fraction than the anterior cartilaginous wall. This hierarchy likely reflects functional specialization: the posterior wall undergoes greater dynamic deformation during respiration and cough, necessitating robust elastic scaffolding. Interestingly, the paired main bronchi showed symmetric age-related changes without clinically significant laterality differences, supporting the systemic nature of elastic fibre aging rather than localized mechanical wear[20].

The validation of quantitative findings through semi-quantitative observer scoring strengthens confidence in the primary results. Despite only fair inter-observer agreement ($\kappa=0.217$), the strong correlations between consensus scores and objective parameters ($r = -0.65$ for elastic area, $r = 0.61$ for fragmentation) confirm that trained observers can reliably detect age-related changes. The dramatic shift from predominantly score 0-1 in young adults to score 2-3 in octogenarians provides visual confirmation of the quantitative deterioration[21].

Several limitations merit consideration. The cross-sectional design cannot establish causality or distinguish age-related changes from cohort effects. Cadaveric specimens may not perfectly represent living tissue mechanics, though fixation protocols were standardized. Incomplete medical histories prevented adjustment for chronic diseases that might accelerate elastic fibre degradation. Post-mortem intervals varied modestly but showed no correlation with measured parameters.

Clinical implications emerge from these anatomical findings. The documented structural fragility of aged airways may inform surgical planning for elderly patients undergoing tracheostomy or bronchoscopic interventions. Understanding baseline age-related changes helps distinguish physiological from pathological findings in diagnostic imaging. Future longitudinal studies tracking individual trajectories could

identify factors that accelerate or protect against elastic fibre loss, potentially revealing therapeutic targets for preserving respiratory function in aging populations.

CONCLUSION

This histomorphometric study demonstrates significant age-related deterioration of elastic fibres in the human trachea and main bronchi, with elastic area fraction declining 29-41% and fragmentation increasing three-fold from young adulthood to advanced age. Strong correlations ($r = -0.79$ to -0.85) confirm age as the dominant determinant, explaining over 84% of structural variance. Regional anatomical hierarchy persists throughout life, with the tracheal posterior wall maintaining superior preservation. Semi-quantitative validation corroborates quantitative findings. These anatomical changes provide mechanistic insight into age-related alterations in airway compliance and respiratory mechanics, with implications for clinical assessment and surgical planning in elderly populations.

Author Contributions: All the authors equally contributed for the study and approved the final draft copy of the publication.

Conflicts of Interests: None

REFERENCES

- [1]. Karakioulaki M, Tzanakis N. Extracellular matrix remodelling in COPD. *Eur Respir Rev.* 2020;29:190124. <https://doi.org/10.1183/16000617.0124-2019> PMID:33208482 PMCID:PMC9488912
- [2]. Burgess JK, Weiss DJ, Westergren-Thorsson G, Wigen J, Dean CH, Mumby S, et al. Extracellular matrix as a driver of chronic lung diseases. *Am J Respir Cell Mol Biol.* 2024;70:239-246. <https://doi.org/10.1165/rcmb.2023-0176PS> PMID:38190723
- [3]. Christopoulou ME, Papakonstantinou E, Stolz D. Matrix metalloproteinases in chronic obstructive pulmonary disease. *Int J Mol Sci.* 2023;24:3786. <https://doi.org/10.3390/ijms24043786> PMID:36835197 PMCID:PMC9966421
- [4]. Saputra PB, Purwati DD, Ulhaq AUD, Yolanda S, Djatioetomo YCED, Rosyid AN, et al. Neutrophil elastase in the pathogenesis of chronic obstructive pulmonary disease: a review. *Curr Respir Med Rev.* 2023;19:29-35. <https://doi.org/10.2174/1573398X18666220929170117>
- [5]. Bhatt SP, Bodduluri S, Reinhardt JM, Nakhmani A, Crapo JD, Silverman EK, et al. Mechanically affected lung and progression of emphysema. *Am J Respir Crit Care Med.* 2025;

- 211:1409-1417.
<https://doi.org/10.1164/rccm.202409-18200C>
PMid:40009041 PMCID:PMC12369868
- [6]. Bhana RH, Magan AB. Lung mechanics: a review of solid mechanical elasticity in lung parenchyma. *J Elast.* 2023; 153:53-117.
<https://doi.org/10.1007/s10659-022-09973-6>
PMid:36619653 PMCID:PMC9808719
- [7]. Heinz A. Elastases and elastokines: elastin degradation and its significance in health and disease. *Crit Rev Biochem Mol Biol.* 2020;55:252-273.
<https://doi.org/10.1080/10409238.2020.1768208>
PMid:32530323
- [8]. De Ryk J, Thiesse J, Namati E, McLennan G. Stress distribution in a three dimensional, geometric alveolar sac under normal and emphysematous conditions. *Int J Chron Obstruct Pulmon Dis.* 2007;2:81-91.
<https://doi.org/10.2147/copd.2007.2.1.81>
PMid:18044070 PMCID:PMC2692121
- [9]. Wang K, Liao Y, Li X, Wang R, Zeng Z, Cheng M, et al. Inhibition of neutrophil elastase prevents cigarette smoke exposure-induced formation of neutrophil extracellular traps and improves lung function in a mouse model of chronic obstructive pulmonary disease. *Int Immunopharmacol.* 2023;114:109537.
<https://doi.org/10.1016/j.intimp.2022.109537>
PMid:36495695
- [10]. Fagiola M, Reznik S, Riaz M, Qyang Y, Lee S, Avella J, et al. The relationship between elastin cross-linking and alveolar wall rupture in human pulmonary emphysema. *Am J Physiol Lung Cell Mol Physiol.* 2023;324:L1-L10.
<https://doi.org/10.1152/ajplung.00284.2022>
PMid:37014816
- [11]. Suki B, Bates JH. Lung tissue mechanics as an emergent phenomenon. *J Appl Physiol.* 2011;110:1111-1118.
<https://doi.org/10.1152/jappphysiol.01244.2010>
PMid:21212247 PMCID:PMC3075131
- [12]. Fessler HE, Macklem PT. Percolation and phase transitions. *Am J Respir Crit Care Med.* 2007;176:1065-1066.
<https://doi.org/10.1164/rccm.200704-557ED>
PMid:17823359
- [13]. Fagiola M, Gu G, Avella J, Cantor J. Free lung desmosine: a potential biomarker for elastic fiber injury in pulmonary emphysema. *Biomarkers.* 2022;27:319-324.
<https://doi.org/10.1080/1354750X.2022.2043443>
PMid:35170389
- [14]. Reichheld SE, Muiznieks LD, Stahl R, Simonetti K, Sharpe S, Keeley FW. Conformational transitions of the cross-linking domains of elastin during self-assembly. *J Biol Chem.* 2014;289:10057-10068.
<https://doi.org/10.1074/jbc.M113.533893>
PMid:24550393 PMCID:PMC3974977
- [15]. Chen YJ, Jeng JH, Chang HH, Huang MY, Tsai FF, Yao CCJ. Differential regulation of collagen, lysyl oxidase and MMP-2 in human periodontal ligament cells by low-and high-level mechanical stretching. *J Periodontol Res.* 2013;48:466-474.
<https://doi.org/10.1111/jre.12028>
PMid:23190051 PMCID:PMC10298483
- [16]. Mecham RP. Elastin in lung development and disease pathogenesis. *Matrix Biol.* 2018;73:6-20.
<https://doi.org/10.1016/j.matbio.2018.01.005>
PMid:29331337 PMCID:PMC6041195
- [17]. Schröder CU, Heinz A, Majovsky P, Karaman Mayack B, Brinckmann J, Sippl W, et al. Elastin is heterogeneously cross-linked. *J Biol Chem.* 2018;293:15107-15119.
<https://doi.org/10.1074/jbc.RA118.004322>
PMid:30108173 PMCID:PMC6166741
- [18]. Stone PJ, Morris SM, Thomas KM, Schuhwerk K, Mitchelson A. Repair of elastase-digested elastic fibers in acellular matrices by replating with neonatal rat-lung lipid interstitial fibroblasts or other elastogenic cell types. *Am J Respir Cell Mol Biol.* 1997;17:289-301.
<https://doi.org/10.1165/ajrcmb.17.3.2597>
PMid:9308916
- [19]. Shifren A, Mecham RP. The stumbling block in lung repair of emphysema: elastic fiber assembly. *Proc Am Thorac Soc.* 2006;3:428-433.
<https://doi.org/10.1513/pats.200601-009AW>
PMid:16799087 PMCID:PMC2658707
- [20]. Shen J, Lin X, Liu J, Li X. Effects of cross-link density and distribution on static and dynamic properties of chemically cross-linked polymers. *Macromolecules.* 2018;52:121-134.
<https://doi.org/10.1021/acs.macromol.8b01389>
- [21]. Liu Y, Xian W, He J, Li Y. Interplay between entanglement and crosslinking in determining mechanical behaviors of polymer networks. *Int J Smart Nano Mater.* 2023;14:474-495.
<https://doi.org/10.1080/19475411.2023.2261777>
- [22]. Mariano CA, Sattari S, Ramirez GO, Eskandari M. Effects of tissue degradation by collagenase and elastase on the biaxial mechanics of porcine airways. *Respir Res.* 2023;24:105.
<https://doi.org/10.1186/s12931-023-02376-8>
PMid:37031200 PMCID:PMC10082978
- [23]. Trêbacz H, Barzycka A. Mechanical properties and functions of elastin: an overview. *Biomolecules.* 2023;13:574.
<https://doi.org/10.3390/biom13030574>
PMid:36979509 PMCID:PMC10046833
- [24]. Burla F, Mulla Y, Vos B, Aufderhorst-Roberts A, Koenderink G. From mechanical resilience to active material properties in biopolymer networks. *Nat Rev Phys.* 2019;1:249-263.
<https://doi.org/10.1038/s42254-019-0036-4>
- [25]. Jamhawi NM, Koder RL, Wittebort RJ. Elastin recoil is driven by the hydrophobic effect. *Proc Natl Acad Sci U S A.* 2024;121:e2304009121.
<https://doi.org/10.1073/pnas.2304009121>
PMid:38442161 PMCID:PMC10945822

How to cite this article: Doni R Praveen Kumar, Arasada Archana, T. Neeraja, K. Lakshmi Kumari, Parvatha Varthine. Age-Related Deterioration of Elastic Fibres in the Human Trachea and Main Bronchi: A Quantitative Histomorphometric Study. *Int J Anat Res* 2026;14(2):9511-9523. DOI: 10.16965/ijar.2026.128